Uphill Drift in the Absence of Current in Single-File Diffusion

Benjamin Sorkin[1] and David S. Dean[2,3,*]
[1]School of Chemistry and Center for Physics and Chemistry of Living Systems, Tel Aviv University, 69978 Tel Aviv, Israel
[2]Université Bordeaux, CNRS, LOMA, UMR 5798, F-33400 Talence, France
[3]Team MONC, INRIA Bordeaux Sud Ouest, CNRS UMR 5251, Bordeaux INP, Université Bordeaux, F-33400 Talence, France

(Received 1 April 2024; accepted 14 August 2024; published 3 September 2024)

Single-file diffusion is a paradigmatic model for the transport of Brownian colloidal particles in narrow one-dimensional channels, such as those found in certain porous media, where the particles cannot cross each other. We consider a system where a different external uniform potential is present to the right and left of an origin. For example, this is the case when two channels meeting at the origin have different radii. In equilibrium, the chemical potential of the particles are equal, the density is thus lower in the region with the higher potential, and by definition there is no net current in the system. Remarkably, a single-file tracer particle initially located at the origin, with position denoted by $Y(t)$, exhibits an average *uphill* drift toward the region of *highest* potential. This drift has the late time behavior $\langle Y(t)\rangle = Ct^{1/4}$, where the prefactor C depends on the initial particle arrangement. This surprising result is shown analytically by computing the first two moments of $Y(t)$ through a simple and physically illuminating method, and also via extensive numerical simulations.

DOI: 10.1103/PhysRevLett.133.107101

Single-file diffusion (SFD) is a model for the dynamics of Brownian particles in a vast range of physical systems where transport is effectively one dimensional. It describes particles with hard-core repulsion that cannot bypass each other, even in the pointlike limit. SFD has been extensively studied from both theoretical [1–16] and experimental [16–23] perspectives. This model plays a pivotal role in characterizing transport in porous media [16] and along the cytoskeleton [17], motion of colloids [18,19], drug delivery devices [20], and even gene regulation [21].

From a theoretical point of view, SFD is an important model for understanding the out-of-equilibrium dynamics of interacting particle systems given its analytical tractability. For a long time it has been known that a tracer particle in SFD exhibits anomalous diffusion, having a mean-squared displacement (MSD) which grows as $t^{1/2}$ [1–3]. This dramatic slowing down of dispersion is due to the dynamical caging effect by the surrounding particles. SFD also exhibits other fascinating statistical phenomena. It shows an everlasting dependence on the statistics of the initial conditions [4,5], as well as a dependence on how the two averages over thermal noise and initial conditions are performed [6,7].

SFD has been extensively studied for homogeneous environments. However, substrates like porous media and DNA strands are inherently inhomogeneous due to varying pore structures and codon sequences. This heterogeneity is exploited in applications, such as tailoring pore sizes for controlled drug release [20] and influencing "obstacle" protein binding rates to affect tracer sliding speed [21]. Thus, investigating SFD in inhomogeneous environments holds significant interest, as it may uncover new useful phenomena.

Only a limited literature addresses SFD with space-dependent external potentials and diffusivities. The few techniques connect the tracer's displacement to the statistics of background particle crossings [7,24–26] or to the distribution of an isolated particle [27–31] for systems that are symmetric about the origin. In these cases, no new SFD-related effects have been observed other than the above, as at late times they either behave like SFD in an homogeneous environment but with a rescaled diffusion constant [7,26,28] or reach the boundaries of a confining potential [28,29]. The surprising phenomenon we discover in this Letter is facilitated by a single step potential arising at the interface between two differing substrates.

To illustrate, shown in Fig. 1(a) is a sketch of an interface between two porous media, where the pore size decreases upon going from the medium on the left (L) to the right (R). From entropic considerations, the equilibrium concentration of colloids per unit length will be higher in medium L. Namely, in the dilute limit, the number of particles within a channel is proportional to the free volume available for a single particle, $L\pi(R_{L/R}-a)^2$, where L is the channels' length and a and $R_{R/L}$ are the radii of the colloid and the corresponding channel. Thus, the mean one-dimensional particle densities in each bulk are $\bar{\rho}_{L/R} \sim (R_{L/R}-a)^2$, which can be recast into a Boltzmann factor with the

*Contact author: david.dean@u-bordeaux.fr

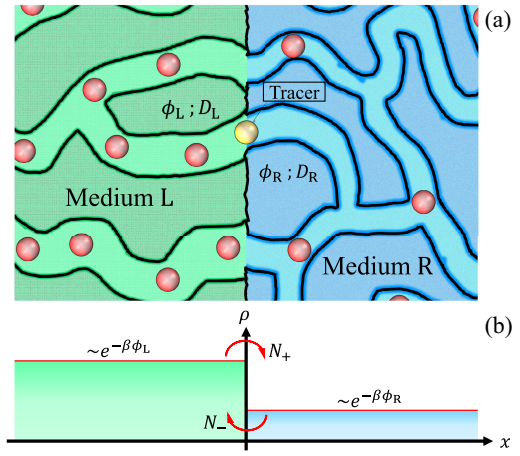

FIG. 1. (a) Illustration of an interface between two particle-laden porous media at steplike equilibrium conditions. The pores are so narrow that particles cannot overtake one another [16]. The pores within medium L (left) are wider than in medium R (right). (b) The average one-dimensional concentration profile $\bar{\rho}(x)$ across the interface. In equilibrium, the medium with the larger pores has the larger particle concentration according to $e^{-\beta(\phi_R-\phi_L)} = (R_R-a)^2/(R_L-a)^2$, where $R_{L/R}$ and a are the pores' and the tracer's radii. The average number of particles crossings from left to right, $\langle N_+\rangle$, and from right to left, $\langle N_-\rangle$, are equal in equilibrium.

effective potential $\phi_{L/R} = -2\beta^{-1}\ln(R_{L/R}-a)$, where $\beta = 1/k_B T$ is the inverse temperature. Therefore, in equilibrium, the mean densities on either side are related via

$$\frac{\bar{\rho}_R}{\bar{\rho}_L} = e^{-\beta(\phi_R-\phi_L)}, \tag{1}$$

as illustrated in Fig. 1(b). A variation in the composition of the surrounding media will also lead to unequal effective potentials, for example, via differences in the Van der Waals interactions. The local diffusion constants, denoted by $D_{L/R}$, will also depend on the local environment, and in particular on the pore radii. We will consider the case of arbitrary values for $\phi_{L/R}$ and $D_{L/R}$ which are taken to be uniform in each bulk [32], thus generating a steplike difference in transport properties to the left and right.

The striking result of this Letter is that, for equilibrium steplike initial condition, the position of the tracer particle $Y(t)$ at late times still has an average drift. Moreover, this drift is toward the region with the *higher* potential, and scales as $\langle Y(t)\rangle \sim t^{1/4}$ and occurs without a macroscopic density current. We prove this result analytically and confirm it by introducing a discrete simulation method that is capable of capturing such late-time dynamics. We also compute the MSD of the tracer and find the SFD scaling $\langle Y^2(t)\rangle_c \sim t^{1/2}$. The numerical prefactors for both the drift and variance can be computed exactly; as in previous studies on SFD in homogeneous systems, they exhibit an everlasting dependence on initial conditions.

Theory—Theoretical approaches for the treatment of free SFD (i.e., no interactions other than the hard-core repulsions) include, e.g., the macroscopic fluctuation theory [7,33–35] and the Bethe ansatz for the full joint probability density function [12,36]. Another, simpler approach adopted here is based on a link between SFD and two independent effusion problems [9,25]. This approach precisely pinpoints the physical mechanism leading to the uphill drift.

The key idea in the approach of Refs. [1,9] is that when single-file particles cross, the hard-core constraint can be imposed by relabeling the particles. This means that if all the particles are assumed to be indistinct, the system appears as if the particles do not interact with each other but only with the externally applied potentials. Each particle in the noninteracting system has a probability density function $p(x,t)$ which evolves according to the Fokker-Planck equation

$$\frac{\partial p(x,t)}{\partial t} = \frac{\partial}{\partial x}\left\{D(x)\left[\frac{\partial p(x,t)}{\partial x} + \beta p(x,t)\frac{d\phi(x)}{dx}\right]\right\}. \tag{2}$$

$D(x<0) = D_L$, $D(x>0) = D_R$, $\phi(x<0) = \phi_L$, and $\phi(x>0) = \phi_R$ represents our model for diffusion of noninteracting particles in two joined channels. Now, if the single-file tracer particle is started at $Y(t) = 0$, then at time t the number of particles to its left is conserved. This can be shown to give the condition [7,25,26,37]

$$\int_0^{Y(t)} dx\rho(x,t) = \int_{-\infty}^{0} dx[\rho(x,0) - \rho(x,t)]. \tag{3}$$

Here, $\rho(x,t) = \sum_{n=1}^{N}\delta(x - X_n(t))$ is the stochastic density field of the N background particles, positioned at $\{X_n(t)\}$.

We first simplify the right-hand side of Eq. (3). We separate the number density field as $\rho(x,t) = \rho_L(x,t) + \rho_R(x,t)$ where, by keeping track of the particle identities, $\rho_L(x,t)$ $[\rho_R(x,t)]$ corresponds to the particles that start in the left (right) medium at $t = 0$. By definition, $\rho_L(x > 0, 0) = 0$ $[\rho_R(x<0,0) = 0]$. Therefore, $N_+(t)$ $[N_-(t)]$, the number of particle that started from the left (right) of the interface at $t = 0$ and appear in the right (left) medium at time t, is given by $N_+(t) = \int_0^\infty dx\,\rho_L(x,t)$ $[N_-(t) = \int_{-\infty}^0 dx\,\rho_R(x,t)]$. Notice that $\int_0^\infty \rho_L(x,t) + \int_{-\infty}^0 \rho_L(x,t) = \int_{-\infty}^0 \rho_L(x,0)$, with which we relate the right-hand side of Eq. (3) to the number of crossings [37],

$$\int_{-\infty}^{0} dx[\rho(x,0) - \rho(x,t)] = N_+(t) - N_-(t). \tag{4}$$

We now consider the left-hand side of Eq. (3) and make the assumption that $|Y(t)|$ becomes large with time. This means that we can apply the law of large numbers to the

left-hand side of Eq. (3) and replace it with its average for a fixed big $Y(t)$ [9,25]. Since the average densities start with their equilibrium values, the average value of $\rho(x,t)$ does not evolve in time and we can write

$$\int_0^{Y(t)} dx\,\rho(x,t) \simeq \bar{\rho}_R Y(t)\Theta[Y(t)] + \bar{\rho}_L Y(t)\Theta[-Y(t)], \quad (5)$$

where Θ is the Heaviside step function. According to the central-limit theorem (CLT), the corrections are $\mathcal{O}[\sqrt{\bar{\rho}_R Y(t)}]$ for $Y(t) > 0$ and $\mathcal{O}[\sqrt{-\bar{\rho}_L Y(t)}]$ for $Y(t) < 0$.

Inserting Eqs. (4) and (5) into Eq. (3), we find the late-time relation between the motion of the single-file tracer and the number of crossings,

$$\bar{\rho}_R Y(t)\Theta[Y(t)] + \bar{\rho}_L Y(t)\Theta[-Y(t)] = N_+(t) - N_-(t). \quad (6)$$

Equation (6) implies that a positive displacement, $Y(t) > 0$, arises from more crossing rightward than leftward, $N_+(t) > N_-(t)$, and vice versa. We use this to rearrange Eq. (6) so as to express $Y(t)$ explicitly in terms of the number of crossings,

$$Y(t) = \frac{[N_+(t) - N_-(t)]}{\bar{\rho}_R}\Theta[N_+(t) - N_-(t)] - \frac{[N_-(t) - N_+(t)]}{\bar{\rho}_L}\Theta[N_-(t) - N_+(t)]. \quad (7)$$

This simple equation elucidates all the phenomena we will discuss in the following. From Eq. (7), we will see that $\langle \mathrm{sign}[Y(t)]\rangle = 0$, corresponding to zero current (the tracer is equally likely to go to the left or right) while the difference in $\bar{\rho}_R$ and $\bar{\rho}_L$ (and the appearance of the functions $\Theta[N_+(t) - N_-(t)]$ and $\Theta[N_-(t) - N_+(t)]$) leads to a nonzero drift. In other words, while the crossings to either right $[N_+(t) > N_-(t)]$ or left $[N_+(t) < N_-(t)]$ occur with the same probabilities at equilibrium, the distance that the tracer moves into each bulk per crossing is bigger in the more dilute region. This point succinctly explains the physical mechanism behind the surprising nonzero tracer uphill drift without current that we report here. The rest of the analysis relies on obtaining the statistics of $Y(t)$ in terms of the two, known, independent statistics of $N_\pm(t)$ [25].

In what follows, we will consider two types of initial conditions. The first is ideal-gas initial conditions, where the system is in perfect equilibrium having identical and independent uniform distribution for all the particles according to each bulk's density [41]. The average over the full statistics of the equilibrium initial configuration in this case will be denoted by $\langle\rangle_{\mathrm{id}}$. The second is perfect crystalline initial conditions, where the particles are set up with the equilibrium densities to the left and right of the origin but are equally spaced in a lattice, whose averages we will denote as $\langle\rangle_{\mathrm{cr}}$. In both cases we write the average initial densities to the left and right in the equilibrium form $\bar{\rho}_{L/R} = \bar{\rho}_0 e^{-\beta\phi_{L/R}}$.

We shall compute the first two moments, $\langle Y(t)\rangle$ and $\langle Y^2(t)\rangle_{\mathrm{c}} = \langle Y^2(t)\rangle - \langle Y(t)\rangle^2$ of the single-file tracer's motion. For the ideal-gas initial conditions, we find [37]

$$\langle Y(t)\rangle_{\mathrm{id}} = [e^{\beta(\phi_R-\phi_L)} - 1]\sqrt{\frac{2}{\bar{\rho}_0}\sqrt{\frac{D_1}{\pi}}}t^{1/4}, \quad (8)$$

$$\langle Y^2(t)\rangle_{\mathrm{c,id}} = \frac{2}{\bar{\rho}_0}\sqrt{\frac{D_2}{\pi}}t^{1/2}, \quad (9)$$

where

$$D_1 = \frac{D_R D_L}{\pi^2[e^{\beta(\phi_R-\phi_L)}\sqrt{D_L} + \sqrt{D_R}]^2}, \quad (10)$$

$$D_2 = D_1\left\{[e^{2\beta(\phi_R-\phi_L)} + 1](\pi - 1) + 2e^{\beta(\phi_R-\phi_L)}\right\}^2. \quad (11)$$

On the other hand, for the crystalline initial conditions (and the quenched statistics [37]) we find the simple relations

$$\langle Y(t)\rangle_{\mathrm{cr}} = \langle Y(t)\rangle_{\mathrm{id}}/2^{1/4}, \quad (12)$$

$$\langle Y^2(t)\rangle_{\mathrm{c,cr}} = \langle Y^2(t)\rangle_{\mathrm{c,id}}/2^{1/2}, \quad (13)$$

which generically appear in SFD problems [4–7]. We see that the drift in both cases is in the direction of the higher potential, thus confirming the phenomenon of uphill drift for *preequilibriated* SFD in the model of connected pores presented here. One should note that according to Eq. (7), in both ideal gas and crystalline cases, $\langle \mathrm{sign}[Y(t)]\rangle = 0$, that is to say the tracer is equally likely to move to the left or right. The effective drift seen is solely due to the lesser crowding in the region of higher potential and thus excursions of the tracer into this region typically go further. This crowding was shown to play a crucial role in the gene expression mechanism [21].

Before proceeding to the simulation, we briefly examine the case of a single isolated particle placed at the origin. The Fokker-Planck equation (2) can be solved [37,42] and the first two moments computed,

$$\langle X(t)\rangle = 2\frac{D_R/D_L - e^{\beta(\phi_R-\phi_L)}}{(D_R/D_L)^{1/2} + e^{\beta(\phi_R-\phi_L)}}\sqrt{\frac{D_L t}{\pi}}, \quad (14)$$

$$\langle X^2(t)\rangle_{\mathrm{c}} = 2\left\{\frac{(D_R/D_L)^{3/2} + e^{\beta(\phi_R-\phi_L)}}{(D_R/D_L)^{1/2} + e^{\beta(\phi_R-\phi_L)}} - \frac{2}{\pi}\left[\frac{D_R/D_L - e^{\beta(\phi_R-\phi_L)}}{(D_R/D_L)^{1/2} + e^{\beta(\phi_R-\phi_L)}}\right]^2\right\}D_L t. \quad (15)$$

Equation (14) shows that a free particle in an infinite system can also drift to the right if $D_R/D_L - e^{\beta(\phi_R-\phi_L)} > 0$, that is, if D_R is sufficiently large. However, a single-file tracer will

always drift toward the region of higher potential at late times, regardless of the values of the diffusivities (assuming both diffusivities are nonzero).

Simulation—Given the rather surprising nature of our analytical predictions, we have performed numerical simulations of both the ideal-gas and crystalline initial conditions. First, note that the relative error due to the CLT decays rather slowly (as $t^{-1/4}$), implying that the finite-time effects are significant [30]. In addition, the discontinuities in $D(x)$ and $\phi(x)$ renders the numerical simulation rather subtle [42]. This pair of challenges is particularly tricky, since we need both extensive numerical simulations to attain the late-time regime as well as a reliable short-ranged smoothing of $\phi(x)$.

To address these issues, we devised an alternative method based on a discrete random walk model that converges to Eq. (2) for small lattice spacing ϵ. (See details in Supplemental Material [37]. There we confirm that the simulation accurately reproduces the isolated particle and particle-crossing statistics.) It has two key advantages. As a lattice model, the discontinuity is just a finite change in $\phi(x)$ and $D(x)$ over a small ϵ. Second, due to the self-similarity of Eq. (2), the spacing can be increased as $\epsilon \sim t_f^{1/2}$ for an arbitrarily long run-time t_f without sacrificing accuracy. Upon simulating many isolated random walkers, the SFD constraint is then simply imposed by sorting their positions [9,25]. To avoid finite sized effects in SFD, the number of background particles must be increased as $t_f^{1/2}$, which is thus the only added cost of a longer simulation. To our knowledge, the simulation used here has not been implemented before. It proves to be considerably faster than the underdamped method of Ref. [42].

Shown in Fig. 2 is the late-time drift and MSD for a single-file tracer for both the ideal-gas and crystalline initial

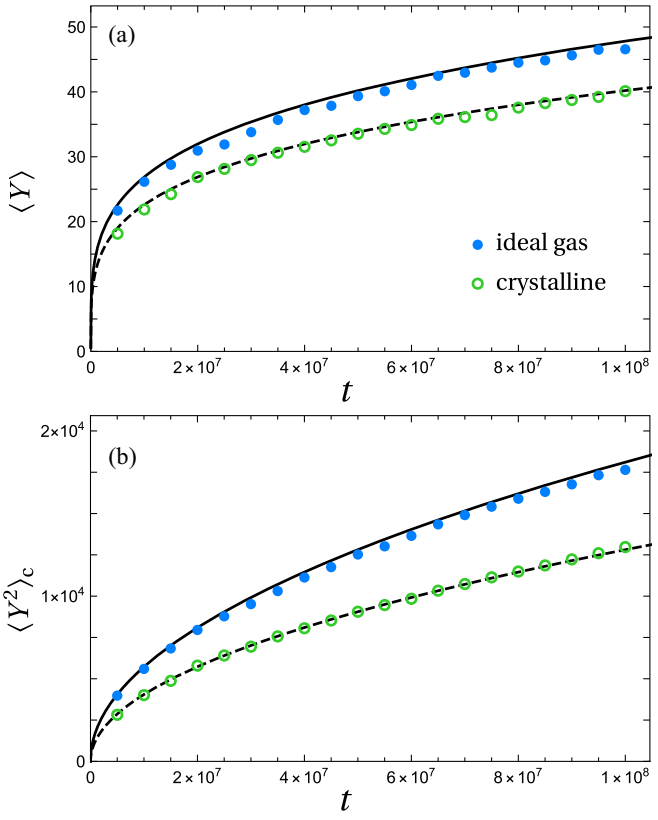

FIG. 2. (a) Drift $\langle Y\rangle$ and (b) mean-squared displacement $\langle Y^2\rangle_c$ for the single-file tracer in the longest simulation, with ideal-gas ("id," blue circles) and crystalline ("cr," empty green circles) initial conditions. The simulation results are depicted by the labels indicated in panel (a), while the immediately adjacent lines are the theoretical predictions [Eqs. (8), (12), (9), and (13)]. Parameter values: $D_L = 1$, $\beta\phi_L = 0$, $\bar{\rho}_L = 1.59$, and $D_R = 2$, $\beta\phi_R = 1$, and $\rho_R = 0.584$. Each data point is obtained from 4×10^4 samples.

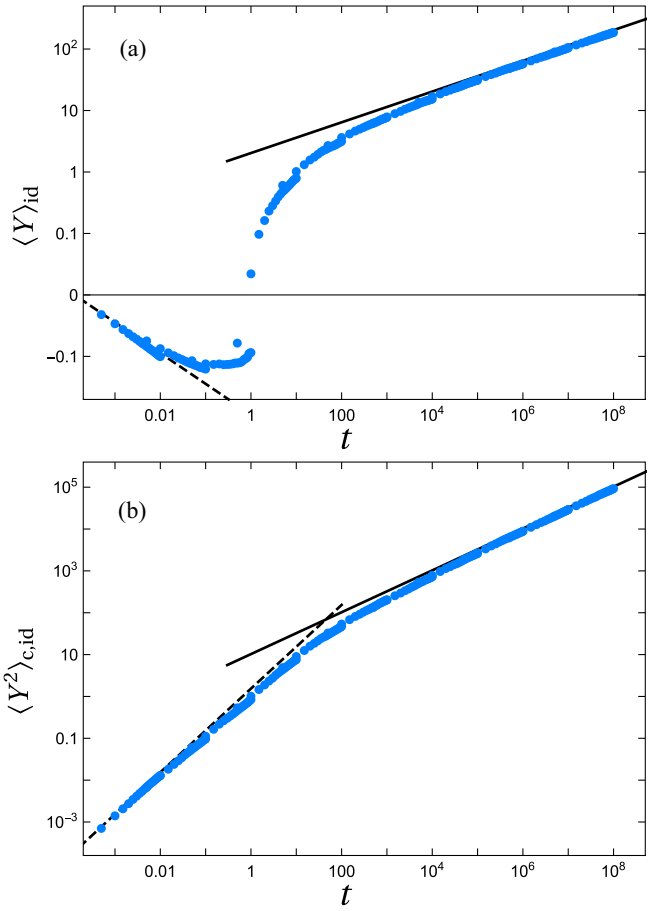

FIG. 3. (a) Drift $\langle Y\rangle_{id}$ and (b) mean-squared displacement $\langle Y^2\rangle_{c,id}$ for single-file tracer with ideal-gas initial conditions across many timescales. The transition from the independent normal diffusion to SFD is clearly seen in the drift turning positive after starting with a negative value. The blue points are given by the simulations, while the black lines are the theoretical predictions for the asymptotic single-file motion [Eqs. (8) and (9)] and the black dashed lines are the theoretical predictions for the diffusion of an isolated particle [Eqs. (14) and (15)]. Parameter values: $D_L = 1$, $\beta\phi_L = 0$, $\bar{\rho}_L = 2.515$, and $D_R = 3$, $\beta\phi_R = 3$, and $\rho_R = 0.125$. Each data point is obtained from 2×10^4 samples.

conditions with $D_R/D_L = 2$ and $\beta(\phi_R - \phi_L) = 1$. The results of the simulation are shown by points, while the analytical late-time predictions, Eqs. (8), (12), (9), and (13), are shown with lines. We see a good agreement with the analytical results in both cases. Most importantly, Fig. 2(a) unequivocally shows the existence of a mean uphill drift.

In Fig. 3 we show the drift and MSD from simulations of ideal-gas initial conditions with $D_R/D_L = 3$ and $\beta(\phi_R - \phi_L) = 3$, over a large range of timescales. At late times, it also demonstrates the convergence to the asymptotic analytical predictions [Eqs. (8) and (9)]. Note that our choices for D_R/D_L and $\beta(\phi_R - \phi_L)$ are a "worse-case scenario" for the uphill (rightward) single-file drift, as an isolated tracer starting at the origin would move downhill (or leftward) according to Eq. (14). Strikingly, indeed the short-time (free-particle-like) drift is negative as shown in Fig. 3(a) along with the theoretical prediction [Eq. (14)], the two being in excellent agreement. Reassuringly, Fig. 3(b) also shows a short-time normal-diffusive regime [which agrees perfectly with Eq. (15), the free-particle MSD]. Thus, the tracer behaves as if it is isolated at short times, and has a downhill bias for these "worse-case scenario" parameters. It is only later that the single-file nature of the problem becomes dominant, at which point the uphill bias kicks in.

Conclusions—We showed that a single-file tracer at the junction between two channels having different potentials and diffusion constants will exhibit an effective late-time drift toward the channel of higher potential. This drift occurs without any associated density current as the probability that the particle moves in either direction is $1/2$. This effect has been shown from both an illuminating theoretical construction as well as a late-time simulation which is particularly useful for SFD on inhomogeneous substrates. Thus, we achieve a situation where, on average, a desired tracer penetrates deeper into the higher-energy bulk without particles accumulating in that medium.

In previous studies spontaneous local drift without flux has been seen for individual Brownian particles with a spatially varying diffusion coefficient, where the so-called spurious drift acts as a real force [43–45]. A phenomenon also referred to as "uphill diffusion" can occur in interacting particle systems when there is a net current toward the region of higher density [46]. The effect seen here is the opposite—motion of particles toward dilute regions (namely, "uphill" here refers to the hill given by the potential). We also note that for SFD in a periodic potential but driven by a constant applied force, a constant drift against the direction of the applied force has been observed in simulations [47,48]. However, the drift reported in this Letter is a purely equilibrium one with a very different temporal dependence.

There are potentially several situations where uphill drift may play a central role, for instance protein crowding may lead to sliding toward target regions on the DNA [21]. In our treatment, we ignored the finite size of the particles, hydrodynamic effects [10,19], and the finite-time corrections [24], which are interesting questions for further theoretical study. Finally, it should be feasible to study such systems experimentally, for instance at the junction of two microfluidic channels.

Acknowledgments—The authors acknowledge useful discussions with Haim Diamant, Eli Barkai, and Tridib Sadhu. D. S. D. acknowledges support from Grant No. ANR-23-CE30-0020-01 EDIPS, and by the European Union through the European Research Council by the EMet-Brown (ERC-CoG-101039103) grant.

[1] T. Harris, Diffusion with, "collisions" between particles, J. Appl. Probab. **2**, 323 (1965).
[2] S. Alexander and P. Pincus, Diffusion of labeled particles on one-dimensional chains, Phys. Rev. B **18**, 2011 (1978).
[3] R. Arratia, The motion of a tagged particle in the simple symmetric exclusion system on Z, Ann. Probab. **11**, 362 (1983).
[4] N. Leibovich and E. Barkai, Everlasting effect of initial conditions on single-file diffusion, Phys. Rev. E **88**, 032107 (2013).
[5] T. Banerjee, R. L. Jack, and M. E. Cates, Role of initial conditions in one-dimensional diffusive systems: Compressibility, hyperuniformity, and long-term memory, Phys. Rev. E **106**, L062101 (2022).
[6] B. Derrida and A. Gerschenfeld, Current fluctuations in one dimensional diffusive systems with a step initial density profile, J. Stat. Phys. **137**, 978 (2009).
[7] P. L. Krapivsky, K. Mallick, and T. Sadhu, Large deviations in single-file diffusion, Phys. Rev. Lett. **113**, 078101 (2014).
[8] F. Spitzer, Interaction of Markov processes, Adv. Math. **5**, 246 (1970).
[9] D. Dürr, S. Goldstein, and J. L. Lebowitz, Asymptotics of particle trajectories in infinite one-dimensional systems with collisions, Commun. Pure Appl. Math. **38**, 573 (1985).
[10] M. Kollmann, Single-file diffusion of atomic and colloidal systems: Asymptotic laws, Phys. Rev. Lett. **90**, 180602 (2003).
[11] T. Bodineau and B. Derrida, Current fluctuations in nonequilibrium diffusive systems: An additivity principle, Phys. Rev. Lett. **92**, 180601 (2004).
[12] S. Prolhac and K. Mallick, Current fluctuations in the exclusion process and Bethe ansatz, J. Phys. A **41**, 175002 (2008).
[13] L. Lizana and T. Ambjörnsson, Single-file diffusion in a box, Phys. Rev. Lett. **100**, 200601 (2008).
[14] P. L. Krapivsky and B. Meerson, Fluctuations of current in nonstationary diffusive lattice gases, Phys. Rev. E **86**, 031106 (2012).
[15] T. M. Liggett, *Interacting Particle Systems* (Springer-Verlag, New York, 1983).
[16] J. Kärger and D. Ruthven, *Diffusion in Zeolites and Other Microporous Solids* (Wiley, New York, 1992).

[17] I. Neri, N. Kern, and A. Parmeggiani, Exclusion processes on networks as models for cytoskeletal transport, New J. Phys. **15**, 085005 (2013).
[18] Q.-H. Wei, C. Bechinger, and P. Leiderer, Single-file diffusion of colloids in one-dimensional channels, Science **287**, 625 (2000).
[19] C. Lutz, M. Kollmann, and C. Bechinger, Single-file diffusion of colloids in one-dimensional channels, Phys. Rev. Lett. **93**, 026001 (2004).
[20] S. Y. Yang, J.-A Yang, E.-S. Kim, G. Jeon, E. J. Oh, K. Y. Choi, S. K. Hahn, and J. K. Kim, Single-file diffusion of protein drugs through cylindrical nanochannels, ACS Nano **4**, 3817 (2010).
[21] G.-W. Li, O. G. Berg, and J. Elf, Effects of macromolecular crowding and DNA looping on gene regulation kinetics, Nat. Phys. **5**, 294 (2009).
[22] B. Lin, M. Meron, Bi. Cui, S. A. Rice, and H. Diamant, From random walk to single-file diffusion, Phys. Rev. Lett. **94**, 216001 (2005).
[23] F. Evers, R. D. L. Hanes, C. Zunke, R. F. Capellmann, J. Bewerunge, C. Dalle-Ferrier, M. C. Jenkins, I. Ladadwa, A. Heuer, R. Castañeda-Priego, and S. U. Egelhaaf, Colloids in light fields: Particle dynamics in random and periodic energy landscapes, Eur. Phys. J. Spec. Top. **222**, 2995 (2013).
[24] T. Sadhu and B. Derrida, Large deviation function of a tracer position in single file diffusion, J. Stat. Mech. (2015) P09008.
[25] D. S. Dean, S. N. Majumdar, and G. Schehr, Effusion of stochastic processes on a line, J. Stat. Mech. (2023) 063208.
[26] B. Sorkin and D. S. Dean, Single-file diffusion in spatially inhomogeneous systems, Phys. Rev. E **108**, 054125 (2023).
[27] J. K. Percus, Anomalous self-diffusion for one-dimensional hard cores, Phys. Rev. A **9**, 557 (1974).
[28] E. Barkai and R. Silbey, Theory of single file diffusion in a force field, Phys. Rev. Lett. **102**, 050602 (2009).
[29] E. Barkai and R. Silbey, Diffusion of tagged particle in an exclusion process, Phys. Rev. E **81**, 041129 (2010).
[30] C. Hegde, S. Sabhapandit, and A. Dhar, Universal large deviations for the tagged particle in single-file motion, Phys. Rev. Lett. **113**, 120601 (2014).
[31] J. Cividini and A. Kundu, Tagged particle in single-file diffusion with arbitrary initial conditions, J. Stat. Mech. (2017) 083203.
[32] This is justified at late times by the rescaling into a uniform constant diffusivity. For details, see the treatments of SFD based on, e.g., the macroscopic fluctuation theory [7,33–35] or a homogenization argument [26,29].
[33] L. Bertini, A. De Sole, D. Gabrielli, G. Jona-Lasinio, and C. Landim, Fluctuations in stationary nonequilibrium states of irreversible processes, Phys. Rev. Lett. **87**, 040601 (2001).
[34] L. Bertini, A. De Sole, D. Gabrielli, G. Jona-Lasinio, and C. Landim, Current fluctuations in stochastic lattice gases, Phys. Rev. Lett. **94**, 030601 (2005).
[35] L. Bertini, A. De Sole, D. Gabrielli, and G. Jona-Lasinio, Non equilibrium current fluctuations in stochastic lattice gases, J. Stat. Phys. **123**, 237 (2006).
[36] C. Rödenbeck, J. Kärger, and K. Hahn, Calculating exact propagators in single-file systems via the reflection principle, Phys. Rev. E **57**, 4382 (1998).
[37] See Supplemental Material at http://link.aps.org/supplemental/10.1103/PhysRevLett.133.107101 for the full derivation of the main result and for further details on the simulation. It includes Refs. [38–40].
[38] S. Torquato, Hyperuniform states of matter, Phys. Rep. **745**, 1 (2018).
[39] B. Øksendal, *Stochastic Differential Equations: An Introduction with Applications* (Springer, Berlin, Heidelberg, 2003).
[40] O. Farago and G. Pontrelli, A Langevin dynamics approach for multi-layer mass transfer problems, Computers in Biology and Medicine **124**, 103932 (2020).
[41] This is justified due to the zero range of the hard-core repulsion.
[42] O. Farago, Algorithms for Brownian dynamics across discontinuities, J. Comput. Phys. **423**, 109802 (2020).
[43] P. Lançon, G. Batrouni, L. Lobry, and N. Ostrowsky, Drift without flux: Brownian walker with a space-dependent diffusion coefficient, Europhys. Lett. **54**, 28 (2001).
[44] G. Volpe and J. Wehr, Effective drifts in dynamical systems with multiplicative noise: A review of recent progress, Rep. Prog. Phys. **79**, 053901 (2016).
[45] G. Volpe, L. Helden, T. Brettschneider, J. Wehr, and C. Bechinger, Influence of noise on force measurements, Phys. Rev. Lett. **104**, 170602 (2010).
[46] M. Colangeli, C. Giberti, and C. Vernia, Uphill diffusions in single and multi-species systems, J. Phys. A **56**, 393001 (2023).
[47] J. Shin, A. M. Berezhkovskii, and A. B. Kolomeisky, Biased random walk in crowded environment: Breaking uphill/downhill symmetry of transition times, J. Phys. Chem. Lett. **11**, 4530 (2020).
[48] A. Ryabov, D. Lips, and P. Maass, Counterintuitive short uphill transitions in single-file diffusion, J. Phys. Chem. C **123**, 5714 (2019).